MOLECULAR AND CELLULAR BIOLOGY, Apr. 1996, p. 1391–1400 Vol. 16, No. 4
0270-7306/96/$04.00+0

Characterization of the Intron-Encoded U19 RNA, a New Mammalian Small Nucleolar RNA That Is Not Associated with Fibrillarin

TAMÁS KISS,[1,2]* MARIE-LINE BORTOLIN,[2] AND WITOLD FILIPOWICZ[1]*

Friedrich Miescher Institute, 4002 Basel, Switzerland,[1] and Laboratoire de Biologie Moléculaire Eucaryote du Centre National de la Recherche Scientifique, Université Paul-Sabatier, 31062 Toulouse Cedex, France[2]

Received 8 November 1995/Returned for modification 6 December 1995/Accepted 6 January 1996

We have characterized a new member (U19) of a group of mammalian small nucleolar RNAs that are not precipitable with antibodies against fibrillarin, a conserved nucleolar protein associated with most of the small nucleolar RNAs characterized to date. Human U19 RNA is 200 nucleotides long and possesses 5′-monophosphate and 3′-hydroxyl termini. It lacks functional boxes C and D, sequence motifs required for fibrillarin binding in many other snoRNAs. Human and mouse RNAs are 86% homologous and can be folded into similar secondary structures, a finding supported by the results of nuclease probing of the RNA. In the human genome, U19 RNA is encoded in the intron of an as yet not fully characterized gene and could be faithfully processed from a longer precursor RNA in HeLa cell extracts. During fractionation of HeLa cell nucleolar extracts on glycerol gradients, U19 RNA was associated with higher-order structures of ~65S, cosedimenting with complexes containing 7-2/MRP RNA, a conserved nucleolar RNA shown to be involved in 5.8S rRNA processing in yeast cells.

The 18S, 5.8S, and 25/28S rRNAs are synthesized in the nucleolus as a single precursor RNA (pre-rRNA) which contains additional sequences that are discarded during RNA maturation. Processing of the pre-rRNA is a complex process involving many RNA intermediates and cleavage events, which frequently follow alternative pathways. The substrate for processing is a large ribonucleoprotein structure containing tens of ribosomal proteins and nucleolar accessory factors associated with nascent pre-rRNA (reviewed in references 10, 53, 60, and 61).

Nucleoli contain a large number of metabolically stable 60- to 260-nucleotide (nt)-long RNA species, referred to as small nucleolar RNAs (snoRNAs) (reviewed in references 13, 14, 37, and 53). Some of these RNAs, e.g., U3, U8, and U13, are transcribed from independent transcription units and contain 5′-terminal trimethylguanosine caps. Most snoRNAs, however, are processed from introns of pre-mRNAs (32; reviewed in references 13, 37, and 52) and contain a monophosphate at the 5′ end (24, 42, 57), consistent with their processing from longer precursor RNAs.

Several snoRNAs have been demonstrated to participate in the processing of pre-rRNA. The U3 snoRNA is involved in the earliest cleavage event, which occurs in the 5′ external transcribed spacer (19, 21, 41), and its depletion impairs the accumulation of mature 18S rRNA in the yeast *Saccharomyces cerevisiae* and vertebrates (19, 50). snoRNAs U14, snR10, and snR30 in *S. cerevisiae* (33, 39, 54) and U22 in *Xenopus laevis* (58) are also essential for 18S rRNA processing, while 7-2/MRP RNA and U8 snoRNA are involved in a maturation of 5.8S rRNA in *S. cerevisiae* (9, 35, 51) and 28S rRNA in *X. laevis* (43), respectively. On the basis of their association with pre-rRNAs or with nascent ribosomal particles, other snoRNAs may also participate in pre-rRNA processing or other aspects of ribosome biogenesis in the nucleolus (1, 2, 14, 37, 53, 60).

The snoRNAs are complexed with proteins, forming small ribonucleoprotein particles (snoRNPs) (reviewed in references 3, 37, and 53). Most of the snoRNPs in yeast and vertebrate cells have a common phylogenetically conserved nucleolar protein, fibrillarin (37, 53, 60). In vertebrates, all snoRNAs of this class contain two short conserved sequence motifs, boxes C (or C′) and D (37, 56, 57), which are essential, either directly or indirectly, for binding of fibrillarin and for RNA accumulation (3, 37, 44).

A small group of nucleolar RNAs that are not associated with fibrillarin comprises 7-2/MRP RNA and three snoRNAs identified recently in vertebrates: U17/E1, E2, and E3. The 7-2/MRP RNA is a component of RNase MRP, which cleaves the pre-rRNA in a region upstream of the 5.8S rRNA in *S. cerevisiae*. The 7-2/MRP RNA is structurally related to the RNA component of RNase P, and both RNAs are associated with the same nucleolar protein, the Th/To antigen (reviewed in references 37 and 40). snoRNAs U17/E1 (8, 24, 48) and E2 and E3 (48) share no obvious structural elements, and the proteins associated with them remain unknown. The function of these snoRNAs has not been established, but the finding that they can be cross-linked to the pre-rRNA (47) suggests that they are involved in ribosome biogenesis. In this work, we report the characterization of a novel non-fibrillarin-associated snoRNA, named U19, identified in human and mouse cells.

MATERIALS AND METHODS

General procedures. Unless indicated otherwise, all techniques used for cloning and sequencing of DNA and for manipulating RNA and oligonucleotides were as described by Sambrook et al. (49). The following oligonucleotides were used in this study: A, GTTTGCACCCAGACTAGGATCAACTCC; B, GAGAGTGGAATGACTCCTGTGGAG; C, ATAGGATCCTGGTCCAGCAGTTGTCAGC; D, TGTAATACGACTCACTATAGGATCCAGCGGTTGTCAGCT; E, AATATTGTTTGCACCCAGACT; F, AGTGCTTGGAGCCAAACCTCAATAA; G, GAUGACUUGAAAGUAGGGC; H, CUUAUCUUGGUGUCACA

* Corresponding author. Mailing address for Tamás Kiss: Laboratoire de Biologie Moléculaire Eucaryote du CNRS, Université Paul-Sabatier, 118 route de Narbonne, 31062 Toulouse Cedex, France. Phone: (33) 61 335934. Fax: (33) 61 335886. Electronic mail address: TAMAS@IBCG.BIOTOUL.FR. Mailing address for Witold Filipowicz: Friedrich Miescher Institute, P.O. Box 2543, 4002 Basel, Switzerland. Phone: (41) 61 6974128 or (41) 61 6976993. Fax: (41) 61 6973976. Electronic mail address: FILIPOWI@FMI.CH.

CAG; I, GTGATCGATCATCCAGCGGTTGTC; and J, CCACTCGAGAAAA AAATTGTTTGCACCTCGACTAG.

Characterization of U19 RNA. HeLa cell nuclear RNA (27) was fractionated by polyacrylamide gel electrophoresis (PAGE) on a denaturing 8 M urea–8% polyacrylamide gel. RNAs migrating between U2 (187-nt-long) and U3 (217-nt-long) snRNAs were recovered and 3′ end labeled with [5′-^{32}P]cytidine 3′,5′-bisphosphate (pCp) and T4 RNA ligase (11). Radiolabeled RNA was again fractionated on an 8 M urea–polyacrylamide gel, and an approximately 200-nt-long RNA, referred to hereafter as U19, was eluted from a gel. Chemical sequencing (28) yielded a sequence of 45 nt proximal to the 3′ end. The middle and 5′-proximal sequence of U19 RNA was determined by dideoxy sequencing, using HeLa cell nuclear RNA as a template and the 5′-end-labeled oligonucleotide complementary to nucleotides 170 to 196 of U19 RNA (oligonucleotide A) as a primer for avian myeloblastosis reverse transcriptase (38). The nature of the 5′-terminal residue was established by cloning of the U19 cDNA. The 3′-terminal sequence of U19 RNA was determined by the oligoribonucleotide ligation-PCR amplification procedure (24). The oligonucleotide corresponding to positions 150 to 168 of the U19 RNA (oligonucleotide B) was used as the upstream primer. Partial cDNAs containing sequences of human and mouse U19 RNAs, lacking four and three 3′-terminal residues, respectively, were generated by a PCR-based procedure which involves tagging of the cDNA 3′ end with an oligonucleotide of known sequence (24). Oligonucleotide A was used as a downstream primer, and the HeLa cell nuclear RNA and mouse NIH 3T3 cell total RNA were used as templates for reverse transcription. PCR-amplified fragments were inserted into the *Sma*I site of pBluescribe, yielding plasmids pHU19/cDNA and pMU19/cDNA. A mouse full-length U19 cDNA was obtained by the oligoribonucleotide ligation-PCR amplification procedure (24), using an oligonucleotide specific to the 5′-terminal region of mouse U19 RNA and containing the *Bam*HI site (oligonucleotide C) as the upstream primer. The amplified fragment was cloned into the *Bam*HI site of pBluescribe, yielding pMU19/cDNAf. The ^{32}P-labeled antisense probe transcribed from pMU19/cDNAf was used for RNase A-RNase T_1 mapping with the NIH 3T3 cell RNA. The resulting protected fragment had a length similar to that of the mouse U19 RNA identified by Northern (RNA) analysis, thus further verifying the sequence of the RNA (data not shown).

To circularize U19 RNA, 10 μg of HeLa nuclear RNA was incubated with 50 U of T4 RNA ligase at 4°C for 48 h in a 500-μl reaction mixture under conditions described by Goodall et al. (15). Half of the RNA sample was gently treated with alkali (29), and RNAs were fractionated on a denaturing 8% polyacrylamide gel. Linear and circular forms of U19 RNA were visualized by Northern analysis using labeled U19 cDNA as a probe. Circularization of the in vitro processed product c was performed as described previously (24).

Secondary structure probing. The coding region of U19 RNA was cloned behind the T7 RNA polymerase promoter by using PCR as follows. The 5′ primer (oligonucleotide D) contained 5′-terminal 18 nt of U19 RNA preceded by the sequence of the T7 RNA polymerase promoter. The 3′ primer (oligonucleotide E) had an 18-nt sequence complementary to the 3′ end region of U19 RNA followed by the *Ssp*I restriction site. HeLa cell DNA was used as a template. The amplified fragment was cloned into the *Sma*I site of pUC19, resulting in pU19cod/T7. In vitro synthesis of U19 RNA was carried out as described previously (15). The resulting U19 RNA transcript contains two additional G residues at the 5′ end and lacks one U residue at the 3′ end.

The 3′ end of the in vitro-synthesized U19 RNA was labeled with [5′-^{32}P]pCp by using T4 RNA ligase (11). The 5′ end was labeled with [γ-^{32}P]ATP and T4 polynucleotide kinase after prior treatment of RNA with calf intestine phosphatase. The RNA was purified by PAGE (6% gel) and used for the secondary structure probing under nondenaturing conditions (10 mM Tris-HCl [pH 7.5], 10 mM $MgCl_2$, 50 mM KCl) as described by Krol and Carbon (30).

Characterization of the human U19 locus. Sequences flanking the U19 RNA coding region in the genome were cloned by inverse PCR (55), using as a template 10 μg of the HeLa cell DNA partially digested with *Sau*3A and circularized by T4 DNA ligase. Oligonucleotides B (see above) and F, complementary to nt 78 to 92 of U19 RNA, were used as primers. Amplified DNA fragments were size fractionated on a 1% agarose gel. Six fragments of increasing length were cloned into the *Sma*I site of pBluescribe. All clones were subjected to sequence analysis. Two cDNA fragments specific for spliced transcripts of the U19 RNA host gene were cloned by reverse transcription-PCR (22). A cDNA obtained by randomly primed reverse transcription of poly(A)$^+$ RNA from HeLa cells was used as a PCR template, and oligonucleotides G and H, specific for exons situated upstream and downstream of the U19 coding region, were used as primers. The primers were selected on the basis of results of RNase A-RNase T_1 mappings performed with HeLa cell poly(A)$^+$ RNA and antisense RNA probes specific for regions flanking the U19 coding sequence (see below).

Southern analysis. HeLa cell DNA (10 μg) was digested with restriction nuclease *Sau*3A, *Dde*I, or *Hae*III and processed as described previously (49). Hybridization to the U19 cDNA probe was carried out in a solution containing 6× SSC (1× SSC is 0.15 M NaCl plus 0.015 M sodium citrate), 50% formamide, 0.5% sodium dodecyl sulfate (SDS), and 100 μg of salmon sperm DNA per ml at 46°C for 18 h. The washing was at 60°C in 0.1× SSC–0.5% SDS.

In vitro processing of U19 RNA. An RNA transcript containing the human U19 RNA sequence, 74 nt of upstream and 107 nt of downstream intronic flanking sequences, and 6 and 2 nt originating from the vector at the 5′ and 3′ ends, respectively (for sequences, see the legend to Fig. 4) was generated from linearized pU17/T7 (25). Processing was carried out in the HeLa cell extract as described previously (24).

Processing of U19 RNA in transfected mouse cells. Plasmids pG_{CXM} and pR have been described elsewhere (25). To obtain pR_M, the coding region of U19 RNA was PCR amplified by using primers I and J, specific for the 5′- and 3′-terminal regions of U19 RNA, respectively. Use of these primers resulted in introduction of a TG-to-GA mutation at positions 186 and 187 of U19 RNA and also led to inclusion of the *Cla*I and *Xho*I sites flanking the mutated U19 RNA coding region (see Fig. 5B). The amplified fragment was inserted between the *Cla*I and *Xho*I sites of pG_{CXM}, yielding pR_M. Transfection of mouse L929 (ATCC CCL1) cells (16) and isolation of RNA (15) were performed as described previously.

Cell fractionation, preparation of extracts, immunoprecipitation, and glycerol gradient analysis. Fractionation of HeLa cells and RNA isolation were performed as described previously (27, 56). To extract nucleolar RNPs, the nucleolar fraction obtained from 3×10^8 HeLa cells was resuspended in 2 ml of extraction buffer containing 10 mM Tris-HCl (pH 7.4), 10 mM NaCl, 10 mM dithiothreitol, 50 μg of yeast tRNA per ml, and 40 U of RNasin per ml. The mixture was incubated on ice for 20 min with occasional shaking and centrifuged for 10 min at 10,000 × *g*. The supernatant was layered on a 10 to 30% glycerol gradient containing 10 mM Tris-HCl (pH 7.4) and 10 mM NaCl and centrifuged at 25,000 rpm for 12 h at 4°C in a TST41 Kontron rotor.

Preparation of HeLa cell extracts and their use for immunoprecipitations of snoRNPs with an antibody against fibrillarin (antibody 72B9 [46]) were performed essentially as described previously (31) except that extraction and immunoprecipitation were done in the presence of 200 mM NaCl. RNA from HeLa subcellular fractions, from glycerol gradient fractions, and from immunoprecipitates was extracted as described previously (26, 27).

RNase A-RNase T_1 mapping. Mapping was performed as described previously (15). Specific complementary RNA probes were synthesized in vitro by T3 or T7 RNA polymerase, using [α-^{32}P]CTP (30 to 40 Ci/mmol) and linearized plasmids as templates. RNA probes used for mapping of human U3, U4, U13, and 7-2/MRP RNAs were as described previously (24, 25, 27). *Eco*RI-linearized pHU19/cDNA served as a template for the preparation of the U19-specific probe. RNase mapping of the in vitro processing products was performed with unlabeled antisense RNA probes as described previously (24). An RNA probe specific to the 3′-end region of U19 RNA was transcribed from *Rsa*I-cut pU19/T7. To obtain a 5′-end-specific probe, the *Eco*RI-*Rsa*I fragment of pU19/T7 was inserted into the *Eco*RI-*Sma*I sites of pBluescribe, and the resulting plasmid, pU19/PR5′, was linearized with *Eco*RI.

Nucleotide sequence accession numbers. Sequences of the human and mouse U19 RNAs are deposited in the EMBL, GenBank, and DDBJ databases under accession numbers X94290 and X94291, respectively.

RESULTS

Characterization of human U19 RNA. A novel snoRNA, named U19, was identified in a nuclear RNA preparation from human HeLa cells, and partial sequence of the 3′ region was obtained by chemical and dideoxy sequencing of RNA. The 3′-terminal sequence, which was not unambiguously established by chemical sequencing, was determined by an oligoribonucleotide ligation-PCR amplification procedure (Fig. 1A). The primary structure of U19 RNA was further confirmed by cloning and sequencing of the U19 cDNA and its genomic locus (see below). Human U19 RNA is 200 nt long (Fig. 1C) and exhibits no significant sequence similarity to any mammalian or yeast snoRNA characterized to date.

Three lines of evidence indicate that the 5′ terminus of U19 RNA is not capped but contains a monophosphate and that a free hydroxyl is present at the 3′ end: (1) antibodies directed against trimethylguanosine or 7-methylguanosine cap structures did not precipitate the RNA (data not shown); (ii) phosphorylation of the 5′ end of U19 RNA in the presence by T4 polynucleotide kinase and [γ-^{32}P]ATP depended upon pretreatment of RNA with calf intestine phosphatase (Fig. 4C and data not shown; and (iii) incubation of U19 RNA with T4 RNA ligase, an enzyme which requires RNA substrates bearing a 5′-monophosphate and 3′-OH termini (11), resulted in formation of a covalently closed circular isoform of the RNA having a characteristic slow mobility in a denaturing gel (Fig. 1B, lane 2). Observations that U19 RNA could be 3′ end labeled with [^{32}P]pCp and tagged with the oligoribonucleotide in T4 RNA

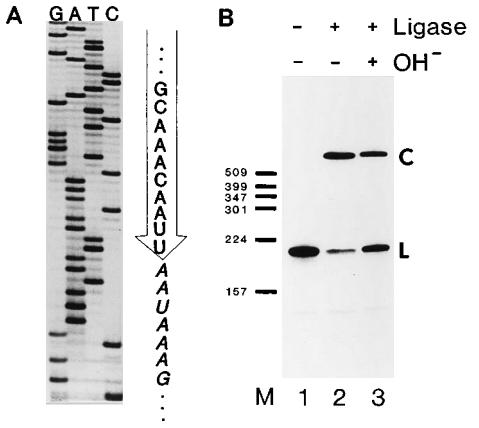

C

pAUCCAGCGGU UGUCAGCUAU CCAGGCUCAU GUGGUGCCUG UGAUGGUGUU ACACUGUUGG AAGAGCAAAC - 70

ACUGUCUUUA UUGAGGUUUG GCUCCAAGCA CUGUUUUGGU GUUGUAGCUG AGUACCUUUG GGCAGUGUUU -140

UGCACCUCUG AGAGUGGAAU GACUCCUGUG GAGUUGAUCC UAGUCUGGGU GCAAACAAUU$_{OH}$ - 200

FIG. 1. Characterization of human U19 RNA. (A) Determination of the 3′-terminal sequence of U19 RNA (shown within an arrow) by the T4 RNA ligase-PCR procedure (see Materials and Methods). The 5′-terminal sequence of the oligoribonucleotide tag ligated to the 3′ end of U19 RNA is shown in italics. (B) U19 RNA is circularized upon treatment with T4 RNA ligase. HeLa cell nuclear RNA was incubated with (lane 2) or without (lane 1) T4 RNA ligase. Lane 3, circularized RNA subjected to mild alkali treatment. RNA samples were fractionated on a 8% denaturing polyacrylamide gel. The blot was probed with labeled U19 cDNA. Positions of linear (L) and circular (C) forms of U19 RNA are indicated on the right. Lane M, size markers (*Hin*fI-digested pBR322). Sizes are indicated in nucleotides. (C) Nucleotide sequence of the human U19 snoRNA.

ligase-catalyzed reactions (see above) also indicate that it contains free 3′ hydroxyl.

A proposed secondary structure for U19 RNA. Since U19 is a nonabundant RNA (see below), an in vitro-transcribed rather than a native RNA was used for probing its structure. The RNA labeled at either the 5′ (Fig. 2A) or the 3′ (Fig. 2B) end was treated under nondenaturing conditions with nucleases specific for either single-stranded (RNases T_1 and A and nuclease S1) or double-stranded (nuclease V1) regions (30). A summary of the structure probing experiments and the derived secondary structure model for U19 RNA are shown in Fig. 2C. The calculated free energy of the proposed RNA structure is −67.5 kcal (ca. −282.4 kJ)/mol. The three major hairpin regions are designated helices I, II, and III. The single-stranded nature of the terminal loops (A, B, and C) and of the major internal bulge-loop structures in the hairpins is well supported by cleavages with the single-strand-specific enzymes. Since nucleotides 148-CUG-150 and 181-UAG-183 in the internal bulge-loop of stem III exhibited reactivity to both single- and double-strand-specific nucleases, it is possible that this region assumes two alternative conformations.

To obtain additional support for the proposed secondary structure, we have characterized a sequence of U19 RNA from mouse NIH 3T3 cells. Mouse RNA (Fig. 2D) has 86% homology with its human equivalent and can be folded into a secondary structure similar to that proposed for human U19 RNA. Sequence differences are found mainly in single-stranded regions (U-1, G-2, G-3, G-30, A-43, G-51, U-68, C-82, C-131, U-168, G-178, and G-183). Most of the alterations in double-stranded regions (e.g., A-10, C-78, C-90, A-132, U-145, and C-147) are compatible with postulated stems, although some changes (e.g., C-40 and C-46) disrupt continuity of short helices. Determination of U19 RNA sequences from other organisms and additional structure probing experiments are required to refine the proposed model.

U19 RNA is encoded within an intron. To determine the structure of the U19 RNA gene, the HeLa cell DNA was digested with restriction endonucleases *Hae*III, *Sau*3A, and *Dde*I and hybridized to the U19 cDNA as a probe. Sequences encoding U19 RNA were found to reside in a single restriction fragment (Fig. 3A). Since, in addition, no evidence of sequence isoforms of U19 RNA was obtained from direct RNA sequencing or during the cloning of human U19 cDNAs, it appears that U19 RNA in humans is encoded by a single-copy gene.

The U19 gene was characterized by inverse PCR using partially digested and circularized HeLa cell genomic DNA. A physical map of the gene, deduced from the sequencing of amplified DNA fragments and supported by the results of additional PCR and RNase A-RNase T_1 mapping analyses (see below; also data not shown), is presented in Fig. 3B. Inspection of the flanking and coding regions of the U19 RNA revealed no upstream or intragenic promoter elements important for transcription of U small nuclear RNA (snRNA), tRNA, or 5S rRNA genes in mammals (17, 62). Hence, U19 RNA may represent a new member of the family of intron-encoded snoRNAs, a possibility supported by the fact that its 5′ end has a monophosphate group, likely a result of its processing from longer precursor RNA (24, 57).

Searching of the databases with sequences of the U19 locus failed to identify the host gene of U19 RNA. However, RNase A-RNase T_1 mapping experiments detected two putative exon regions situated upstream and downstream of the U19 coding region (see the legend to Fig. 3B). Using reverse transcription-PCR, we identified two alternative donor splice sites and the acceptor splice site upstream and downstream of the U19 coding region, respectively (Fig. 3B). The sequences of the 157- and 245-nt-long amplified cDNA fragments representing two alternatively spliced RNAs were identical with the sequence of genomic DNA, indicating that the cDNAs originate from the U19 locus. Both cDNA sequences contain multiple translation termination signals in all three reading frames (unpublished observation). This finding suggests that the intron harboring the U19 sequence is located in the region flanking the protein-coding sequence or that the transcript of the U19 RNA host gene does not code for the protein (58, 59).

In vitro processing of U19 RNA. An internally ^{32}P-labeled RNA transcript containing the U19 RNA region flanked by upstream and downstream intron sequences was incubated with the HeLa cell extract (Fig. 4A). Several RNA products, accumulating in a time-dependent fashion, were identified. Their structures were determined by RNase A-RNase T_1 mapping using unlabeled RNA probes complementary to either the 5′ or 3′ portion of the processing substrate (Fig. 4B). Two major products, a5′ and a3′, accumulating early were found to correspond to RNA processed at only the 5′ and 3′ ends, respectively. The presence of such products indicates that processing reactions at both ends are independent of each other. Product b, appearing after 20 min of incubation, represents RNA fully processed at the 5′ end but still containing a short 3′-trailer sequence similar to that present in the product a3′. The end product of the in vitro processing reaction, product c, comigrated in a denaturing gel with the authentic U19 RNA purified from HeLa cells (Fig. 4C). Incubation of product c with T4 RNA ligase resulted in its circularization (lane 3). These results show that product c represents faithfully processed U19 RNA bearing 5′-monophosphate and 3′-OH termini. The ladder of bands seen between products b and c indicates that the 3′ trailer in product b is 9 nt long and that it is progressively removed by exonucleolytic activity.

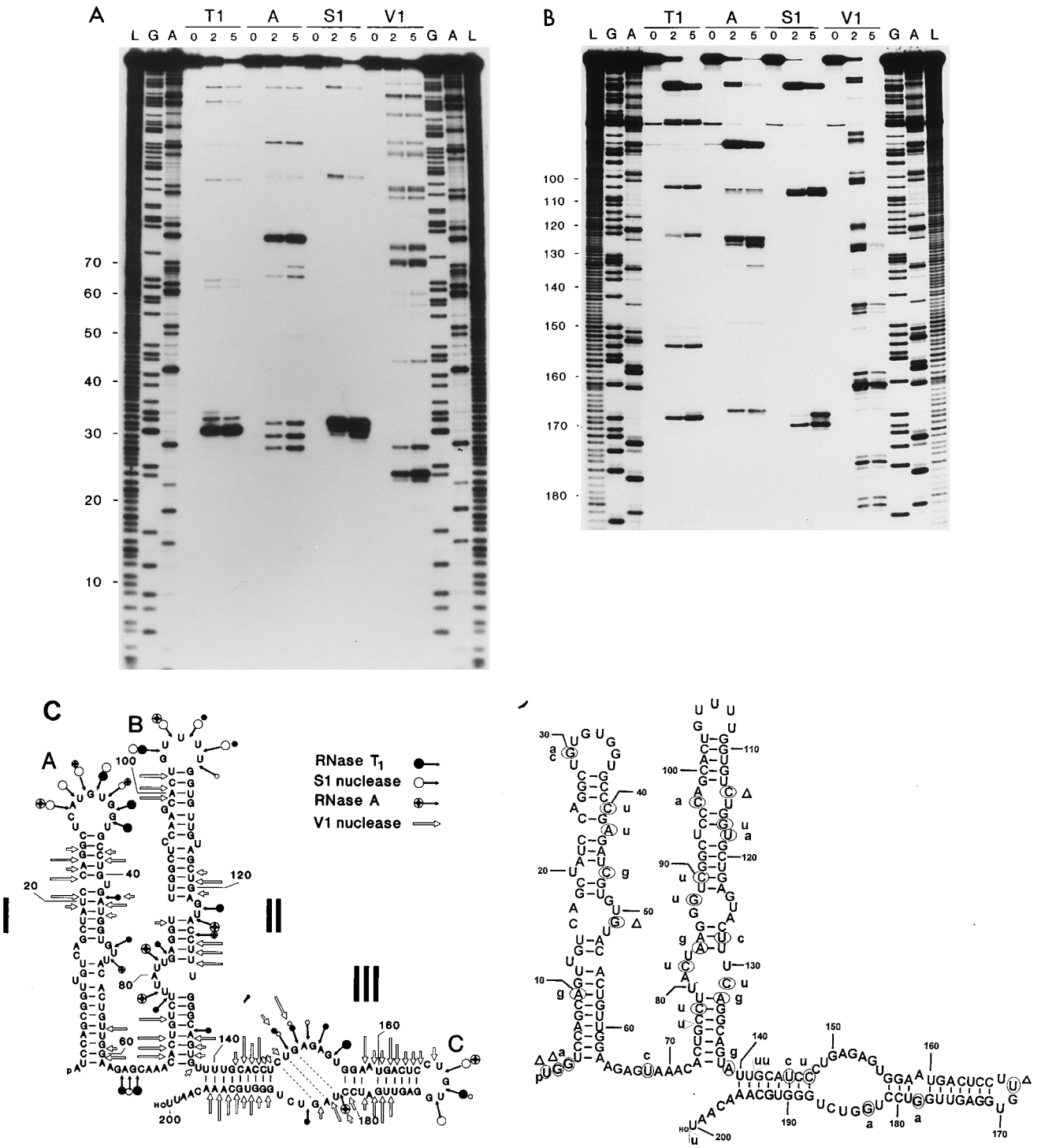

FIG. 2. Nuclease probing of human U19 snoRNA structure. (A and B) Enzymatic cleavage of 5′-end-labeled (A) and 3′-end-labeled (B) U19 RNA transcripts. The U19 transcript was synthesized in vitro; it contains two additional G residues at the 5′ terminus, and one U residue was deleted from the 3′ end to facilitate labeling of the RNA with [^{32}P]pCp (11). RNA was subjected to a limited digestion, under nondenaturing conditions, with RNase T_1 (T1), A (A), or V1 (V1) and nuclease S1 (S1). Incubation times (minutes) are shown above the lanes. Guanosine- and adenosine-specific ladders (lanes G and A, respectively) were produced by partial digestions of U19 RNA with RNase T_1 or RNase U_2 under denaturing conditions. Lanes L, alkaline hydrolysis ladders. RNA fragments were resolved by denaturing PAGE (8% gel). Only two representative autoradiograms are shown; they do not illustrate all cleavages incorporated into the model shown in panel C. Sizes are indicated in nucleotides. (C) Proposed secondary structure of human U19 RNA. Nucleotides accessible to nuclease attacks are marked by nuclease-specific symbols. Sizes of symbols are proportional to the observed nuclease reactivity. (D) Sequence and proposed secondary structure of mouse U19 RNA. Nucleotides different from human U19 RNA are encircled; corresponding residues in human RNA are in lowercase. △, residues missing in human RNA.

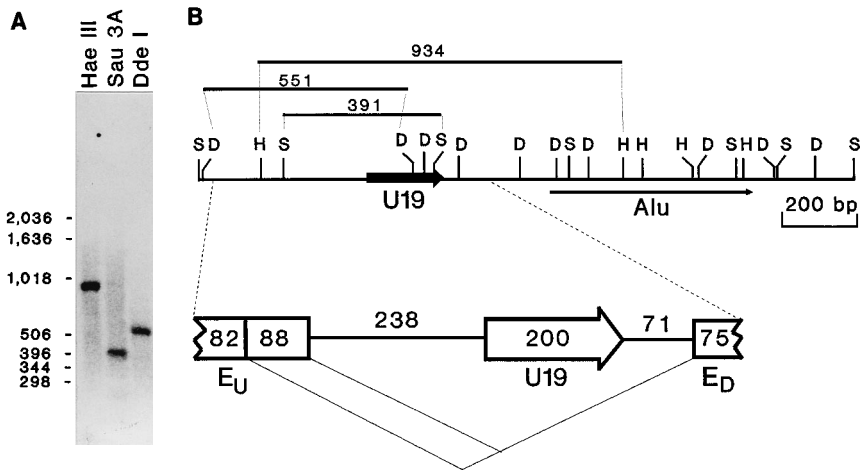

FIG. 3. Organization of the U19 RNA locus. (A) Southern analysis. Genomic DNA isolated from HeLa cells was digested with restriction enzymes indicated above the lanes. The U19 cDNA was used for probing of the blot. Note that electrophoretic mobility of the hybridizing fragments corresponds to the expected 934-bp *Hae*III, 391-bp *Sau*3A, and 551-bp *Dde*I U19-specific fragments diagrammed in panel B. Additional fragments, derived from cleavages by *Dde*I and *Sau*3A in the U19 coding region, have complementarity to the U19 cDNA probe too short to be visualized by Southern analysis. Sizes are indicated in nucleotides. (B) Restriction map of the U19 locus. The U19 RNA coding region and an *Alu* repetitive element are indicated by thick and thin arrows, respectively. The sizes of the U19-specific fragments visualized in Southern analysis (A) are indicated above the map. S, *Sau*3A; D, *Dde*I; H, *Hae*III. Structure of the host intron of human U19 RNA is schematically presented below the genomic map. The upstream (E_U) and downstream (E_D) exon regions were originally identified by RNase A-RNase T_1 mapping using HeLa cell poly(A)$^+$ RNA and ^{32}P-labeled antisense RNA probes originating from the 223-bp upstream and 337-bp downstream *Sau*3A fragments, immediately flanking the *Sau*3A fragment containing most of the U19 coding sequence. Exact positions of the splicing donor and acceptor sites were determined by cloning and sequencing of cDNAs specific for processed transcripts of the U19 host gene (see Materials and Methods). Sequences of two alternative donor sites are TTTTCAG/GTAAATAT (upstream) and ATGGGAG/GTAAATTA (downstream); the sequence of the acceptor site is TGAATCCTAG/ATGCCTT.

In addition to major processing products described above, two minor RNA products, a3′* and a5′(3′*), were observed (Fig. 4A). These products contain unprocessed and fully matured 5′ end, respectively. Mapping with the 3′ probe showed that both these products retain the 45-nt-long trailer sequence (Fig. 4B). The 3′-terminal region in products a3′* and a5′(3′*) has the potential to form an 11-bp hairpin (see the legend to Fig. 4A), which could cause pausing of an exonuclease involved in processing of the RNA (25).

U19 RNA is not associated with fibrillarin. Most of vertebrate snoRNAs are complexed with fibrillarin, and particles of which they are a part are precipitable with antifibrillarin antibodies. Unlike the control fibrillarin-associated U3 snoRNA, the U19 RNA was found predominantly among RNAs recovered from the supernatant of the immunoprecipitation reaction (Fig. 5A). Traces of U19 RNA detected in the immunoprecipitate may represent a small fraction of U19 RNP associated with other, fibrillarin-containing snoRNPs. Autoimmune antibodies against the Th/To antigen, associated with the nucleolar 7-2/MRP RNA, also did not precipitate the U19 RNA (data not shown).

Of the two conserved sequence elements, box C (or C′) and box D, essential for binding of fibrillarin (3, 18, 44, 57), human and mouse U19 RNAs lack box C, but both RNAs contain a short motif (GUCUGG; positions 183 to 188 and 184 to 189 in human and mouse RNAs, respectively), the sequences and positions of which are similar to those of genuine D boxes (consensus RUCUGA [56, 57]). To determine whether the D-like box motif in U19 RNA is of functional importance, we tested the effects of mutations in this sequence on processing of U19 RNA in vivo. The GUCUGG sequence was mutated to GUCGAG, which diverges from the D box consensus in three 3′-proximal positions (point mutations in all of these positions were previously shown to affect accumulation of U14 RNA in yeast cells [18]). The wild-type and mutant U19 sequences were inserted into the second intron of the human β-globin gene (25), and resulting constructs were expressed in transfected mouse L929 cells. Accumulation of U19 RNA and of globin mRNA was assayed by RNase mapping using probes specific for each transcript. As shown in Fig. 5B, control and mutant U19 RNAs were processed from globin pre-mRNA with similar efficiencies (lanes 4 and 10), yielding RNAs identical in size to the authentic HeLa cell U19 RNA (lanes 2 and 7).

U19 RNA is associated with 65S higher-order structures in the nucleolus. HeLa cells were fractionated into cytoplasmic, nuclear, nucleoplasmic, and nucleolar fractions, and RNA isolated from each fraction was analyzed by RNase mapping using probes specific for U19 RNA and, as controls, probes specific for U13 snoRNA and U4 spliceosomal snRNA (Fig. 6A). The U19 RNA, like U13 snoRNA (56), cofractionated with the nucleolar fraction, while U4 snRNA was mainly found in the nucleoplasm. Taking the previously reported copy number of U4 RNA in HeLa cells (200,000 copies per cell [45]) as a reference, the abundance of U19 RNA was estimated as 12,000 copies per cell.

In mammalian cells, snoRNAs U3, U8, U13, and U17 and 7-2/MRP RNA were shown to be associated with two different forms of RNPs (12, 25, 27, 37, 56). Complexes sedimenting at 10S to 20S represent monomeric snoRNPs, while larger structures, sedimenting at 40S to 80S, probably correspond to snoRNPs bound to ribosomal particles undergoing maturation in the nucleolus. To analyze the U19 RNA-specific complexes, HeLa cell nucleolar extracts were fractionated on a 10 to 30% glycerol gradient. In addition to being present in the monoparticle-like fraction of 10S to 15S, the U19 RNA was found in association with higher-order structures of ~65S. For two other nucleolar RNAs analyzed as controls, the 7-2/MRP RNA was also reproducibly found in complexes sedimenting at ~65S, while U3 snoRNA was present in structures of ~80S (56). (Note that during similar analysis performed with total

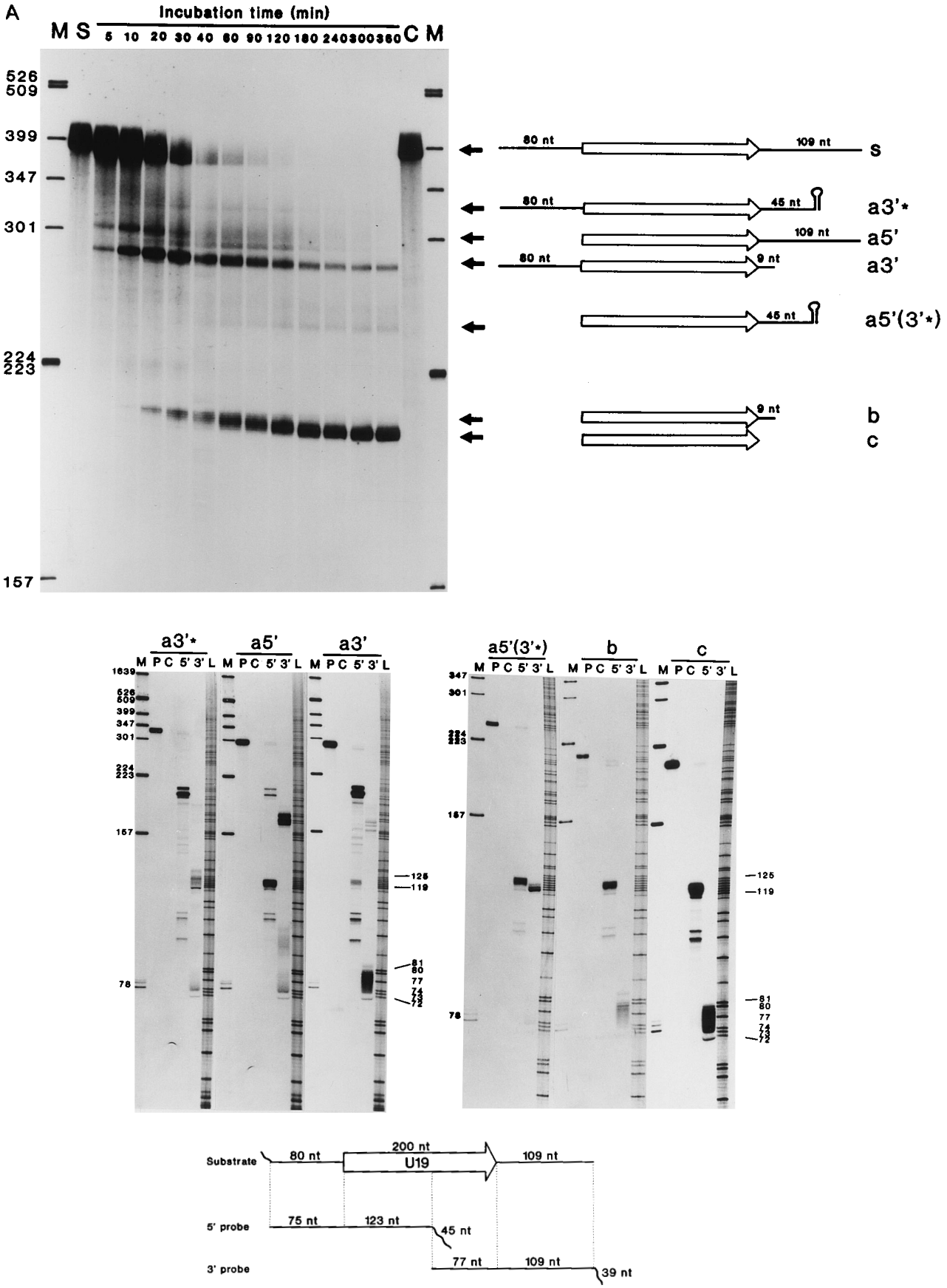
A
Incubation time (min)
M S 5 10 20 30 40 60 90 120 180 240 300 360 C M
526
509
399
347
301
224
223
157
80 nt
109 nt
S
80 nt
45 nt
a3'*
109 nt
a5'
80 nt
9 nt
a3'
45 nt
a5'(3'*)
9 nt
b
c
a3'*
a5'
a3'
a5'(3'*)
b
c
M P C 5' 3' L
1639
526
509
399
347
301
224
223
157
78
125
119
81
80
77
74
73
72
Substrate
200 nt
U19
80 nt
109 nt
5' probe
75 nt
123 nt
45 nt
3' probe
77 nt
109 nt
39 nt

FIG. 4.

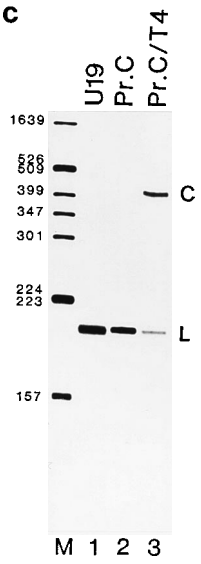

FIG. 4. In vitro processing of U19 RNA. (A) Time-dependent processing of internally labeled 389-nt-long U19/T7 RNA in the HeLa cell S-100 extract. Aliquots were taken at intervals of 5 to 360 min, and RNA was fractionated on a 6% sequencing gel. Lanes S and C, substrate RNA incubated in the absence of the extract for 0 and 360 min, respectively. Sequences flanking the U19 RNA region in the U19/T7 substrate on the 5′ and 3′ sides are gggcgaAUUCAACUG AUACGUCUUCUACCUGGAGUGCCUAGGUAUCUGAAACAAAUAAU GAGAAAGCUGUUUCAGGAAUC. . . and . . .UUUUUCUGUUUGCAGA AAAAGACAGGUUGUCUUAGGGACAGCCUGUCAUUCUUUACCUC UUUGAAUCCUAGAUGCCUUCACCUGAAUGACAUCUACCUCCAUC AGGAtc, respectively. Nucleotides originating from the cloning vector are in lowercase, and those forming a potential hairpin (see text) are underlined. Lanes M, size markers. Schematic structure of the processing substrate and of the products characterized by RNase mapping (B) are shown on the right. (B) Characterization of the 5′ and 3′ ends of the in vitro processing products by RNase A-RNase T_1 mapping using unlabeled antisense RNA probes. Schematic structures of RNA probes and expected sizes of the protected fragments are shown at the bottom. Lanes P, aliquots of purified products, indicated at the top, used for RNase A-RNase T_1 mapping; lanes C, control mappings without added probe; lanes 5′ and 3′, mappings with 5′ and 3′ probes, respectively; lanes M and L, size markers (the latter corresponding to G sequencing ladder). Products a3′* and a5′ were obtained after 30 min of incubation, while others were obtained after 2 h of incubation. These products were isolated from a preparative gel similar to the one shown in panel A. Products c and b were not well separated from each other in the preparative gel. Each of them is a mixture of molecules bearing short (up to approximately 10 nt) 3′ trailers, consistent with the data shown in panel A. Note that mapping of product a3′ with the 3′-end-specific probe yielded a similar protection pattern, indicating that removal of the 3′ trailer sequence may start before the processing of U19 RNA at the 5′ end is completed. (C) Processing product c (lane 2) comigrates in a denaturing gel with the authentic U19 RNA (lane 1) and undergoes circularization upon incubation with the T4 RNA ligase (lane 3). Human U19 RNA was purified by hybrid selection, treated with calf intestine phosphatase, and 5′ end labeled with T4 polynucleotide kinase in the presence of [γ-^{32}P]ATP. To isolate product c used in this experiment, the processing reaction was fractionated by high-resolution denaturing PAGE (12% polyacrylamide gel). Sizes are indicated in nucleotides. L and C, linear and circular forms of RNA.

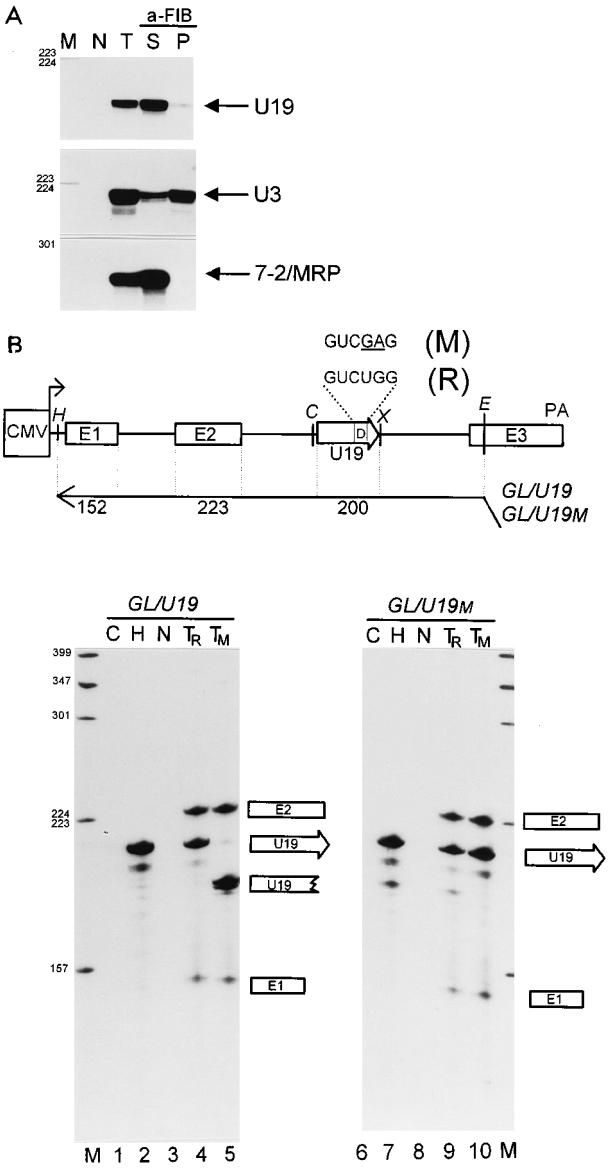

FIG. 5. Human U19 RNA is not precipitable with antifibrillarin antibodies and lacks functional C and D boxes. (A) Immunoprecipitation of snoRNAs from the HeLa cell extract with antifibrillarin (a-FIB) antibodies. RNA recovered from the pellet (lane P) and the supernatant (lane S) of the immunoprecipitation reaction or from the pellet of precipitation with a control nonimmune serum (lane N) was mapped with antisense probes specific for snoRNAs indicated on the right. Lane T, mapping of RNA isolated from HeLa cell extract not subjected to immunoprecipitation. Lane M, size markers. (B) Processing of U19 RNA from the second intron of human β-globin pre-mRNA expressed in mouse cells. Schematic structures of expression constructs containing wild-type U19 RNA sequence (construct R) and U19 sequence bearing mutations in the putative box D are indicated at the top. Abbreviations for restriction sites: H, *Hin*dIII; C, *Cla*I; X, *Xho*I; E, *Eco*RI. The promoter region (cytomegalovirus [CMV]) and the site of polyadenylation (PA) are also indicated. Antisense RNA probes with the expected lengths of protected fragments are shown below. RNA extracted from cells transfected with expression constructs carrying wild-type (lanes T_R) and mutant (lanes T_M) U19 RNAs or RNA from mock-transfected cells (lanes N) were subjected to RNase A-RNase T_1 mapping using probes specific for wild-type (GL/U19) or mutant (GL/U19M) U19 RNA. Lanes C and H, control mappings with 2.5 μg of *Escherichia coli* tRNA and 0.5 μg of HeLa cell RNA, respectively. Positions and structures of protected fragments are shown on the right. Note that the mismatch between the wild-type U19 RNA and the GL/U19M probe is not cleaved by RNases. Sizes are indicated in nucleotides.

cell and not nucleolar extracts, the 7-2/MRP RNA sediments at ~80S [27] [see the legend to Fig. 6].)

DISCUSSION

Most of the vertebrate snoRNAs characterized to date contain two short, conserved sequence elements referred to as boxes C and D, required for accumulation of the RNAs and also, directly or indirectly, for binding of fibrillarin. Apart from the 7-2/MRP RNA, only three vertebrate snoRNAs, U17/E1, E2, and E3, have been reported to lack the C and D boxes (8, 24, 48). In *S. cerevisiae*, the family of snoRNAs apparently lacking these two elements is more complex; however, many of

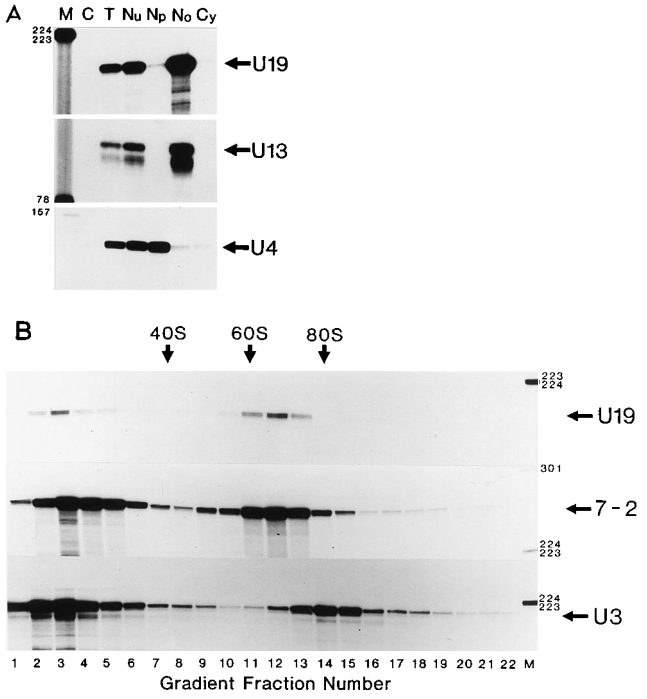

FIG. 6. U19 RNA has nucleolar localization and is associated with 65S higher-order complexes. (A) Subcellular localization of U19 RNA in HeLa cells. RNA (50 ng) extracted either from HeLa cells (lane T) or from nuclear (lane Nu), nucleoplasmic (lane Np), nucleolar (lane No), or cytoplasmic (lane Cy) fractions of HeLa cells was analyzed by RNase mapping using probes specific for U19, U13, or U4 RNA. Lane C, control mappings with *E. coli* tRNA; lane M, size marker. The autoradiography of mappings with the U13 and U19 probes was for 20 h, and that with the U4 probe was for 2 h. To calculate the abundance of U19 RNA, corrections were made for different numbers of labeled C residues present in different probes. (B) Fractionation of the HeLa cell nucleolar extract on a 10 to 30% glycerol gradient. RNA was isolated from each of the 22 fractions and analyzed by RNase mapping using antisense RNA probes specific for U19, 7-2/MRP, or U3 RNA, as indicated on the right. Positions of the HeLa cell 40S, 60S, and 80S ribosomes, run in a parallel gradient, are indicated. Lane M, size marker. Sizes are indicated in nucleotides. Association of 7-2/MRP RNA with ~65S structures was confirmed in five independent experiments. However, it should be noted that previous analysis, performed with total cell and not nucleolar extracts, indicated that 7-2/MRP RNA sediments with ~80S and not ~65S structures (27). Factors responsible for the differences in sedimentation properties, seen with two different extracts, are not known.

them are precipitable with antifibrillarin antibodies (reviewed in reference 37). In this study, we characterized a novel mammalian snoRNA, U19, which is not precipitable with antifibrillarin antibodies. The human and mouse U19 RNAs show 86% identity and have no significant sequence similarity to any of the snoRNAs so far characterized. The proposed secondary structure of U19 RNA, derived by partial digestion of the U19 RNA with different nucleases, also differs from structures proposed for other snoRNAs. The U19 RNA does not have a box C motif, and the presence of a D-like box sequence, GUCU GG, near the 3′ end of U19 RNAs appears to be fortuitous, since its mutation has no effect on processing and accumulation of the RNA in transfected mouse cells. An intact D box was previously shown to be required for accumulation of U14 RNA in yeast cells (18) and U8 RNA in *Xenopus* oocytes (44). Box D, together with other sequences and bound proteins, most probably forms part of the processing signal required for maturation of fibrillarin-associated intronic snoRNAs (2, 6, 36, 37).

In vertebrates, most of the known snoRNAs are encoded within introns of protein-coding genes. These RNAs are not independently transcribed but are processed from introns of the host pre-mRNA (13, 32, 37, 52). Several lines of evidence demonstrate that U19 RNA is a member of the family of intron-encoded snoRNAs. (1) U19 RNA contains a monophosphate at the 5′ end, consistent with it being processed from a longer precursor RNA. (2) At the U19 genomic locus, the U19 RNA sequence is located within the intron of an as yet not fully characterized gene. (3) U19 RNA can be processed from a heterologous intron in transfected simian (25) or mouse (this work) cells. (4) U19 RNA is also faithfully processed in vitro from a longer intronic transcript, resulting in an RNA containing the 5′-monophosphate and 3′-OH termini. (5) From previous experiments (25) and this work (Fig. 4), the processing of U19 RNA appears to be catalyzed by the 5′→3′ and 3′→5′ exonucleases, with the nucleotides immediately adjacent to the mature 3′ end being removed relatively slowly. This processing pathway is similar to that established for two other intron-encoded snoRNAs, U17 (7, 24, 25) and U15 (57, 59). Since non-fibrillarin-associated snoRNAs other than U17 and U19 also do not contain the 5′-terminal cap (42), it is likely that all known members of this group of RNAs in vertebrates are intron encoded.

The coding regions of intronic snoRNAs appear to contain all information necessary for their faithful processing from host introns (25, 36, 37). Many of the fibrillarin-associated intronic snoRNAs contain the helix-bulge-helix structures encompassing the C and D boxes and bringing together the 5′ and 3′ termini of the RNA (2, 57). These structures, together with associated proteins, probably act as processing signals arresting the progress of exonucleases (2, 6, 36, 37). On the basis of the proposed secondary structure model, the 5′ and 3′ ends of U19 RNA are not base paired to each other. Other non-fibrillarin-associated snoRNAs (reference 8 and our unpublished observations), as well as some of the fibrillarin-associated snoRNAs (1), also lack the potential to form a terminal helix. Therefore, different structural elements must be responsible for processing of these snoRNAs. The structure of U19 RNA determined in this study will be of help in defining signals required for its maturation.

Many of the fibrillarin-associated snoRNAs contain long (up to 21 nt) sequences having complementarity to phylogenetically conserved regions in 18S or 25/28S rRNA (reviewed in references 1 and 2). In the case of U14 RNA, the complementarity was shown to be essential for pre-rRNA processing in *S. cerevisiae* (34). A shorter complementary interaction, with the 5′ external transcribed spacer, was also demonstrated to be important for the function of U3 snoRNA in *S. cerevisiae* (5). Non-fibrillarin-associated RNAs U17, E2, and E3 do not generally contain long conserved sequences with the potential to base pair to pre-rRNA (8, 24, 47). Interestingly, the U19 RNA has a potential to base pair with the 5′ end of 5.8S rRNA. In humans, the sequence of 13 nt in U19 RNA (positions 143 to 145) can form 12 bp with 5.8S rRNA residues 3 to 15:

```
5.8S rRNA 5′-ACUCUUACGGUG-3′
                |||||||  ||||
U19 RNA   3′-UGAGAGUUCCAC-5′
```

Similar 12-of-13 complementarity can also be drawn for mouse U19 and 5.8S RNAs. The significance of this observation, if any, is to be established.

Fractionation of HeLa cell nucleolar extracts on glycerol gradients revealed that, in addition to being present in monomeric snoRNPs of 10S to 15S, the U19 RNA is associated with higher-order structures sedimenting at ~65S. Preribosomal particles sedimenting at 65S and containing a precursor of 28S

rRNA, several ribosomal proteins, and ribocharin, an isoelectric variant of the B23 protein (61) which transiently associates with maturing ribosomes, were previously identified in *Xenopus* oocytes (20). The nucleoplasmic localization of *Xenopus* particles suggests that they represent immediate precursors of cytoplasmic 60S subunits on their way to the cytoplasm. The U19 RNA-containing complexes identified in the present work may represent precursors of 60S subunits still associated with the nucleolus, a possibility supported by the finding that 7-2/MRP RNA is also present in complexes of similar size. In yeast cells, 7-2/MRP RNA is involved in the maturation of the large ribosomal subunit, catalyzing the processing of 5.8S rRNA, and it is likely that this RNA has a similar function in vertebrate cells (reviewed in references 37 and 40).

In summary, we have identified in mammalian cells a further U snoRNA which is not associated with fibrillarin. It will be interesting to establish whether snoRNAs belonging to this group share structural properties and interact with common proteins. Likewise, it will be important to characterize signals essential for processing of these snoRNAs from pre-mRNA introns and to define their role in ribosome biogenesis.

ACKNOWLEDGMENTS

We thank E. S. Maxwell, K. Tycowski, and J. A. Steitz for sharing unpublished results, and we thank F. Dragon and P. King for critical reading of the manuscript.

REFERENCES

1. **Bachellerie, J.-P., B. Michot, M. Nicoloso, A. Balakin, J. Ni, and M. J. Fournier.** 1995. Antisense snoRNAs: a family of nucleolar RNAs with long complementarities to rRNA. Trends Biochem. Sci. **20:**261–264.
2. **Bachellerie, J.-P., M. Nicoloso, L.-H. Qu, B. Michot, M. Caizergues-Ferrer, J. Cavaille, and M. H. Renalier.** Novel intron-encoded small nucleolar RNAs with long sequence complementarities to mature rRNAs involved in ribosome biogenesis. Biochem. Cell Biol., in press.
3. **Baserga, S. J., and J. A. Steitz.** 1993. The diverse world of small ribonucleoproteins, p. 359–382. *In* R. F. Gesteland and J. F. Atkins (ed.), The RNA world. Cold Spring Harbor Laboratory Press, Cold Spring Harbor, N.Y.
4. **Baserga, S. J., X. W. Yang, and J. A. Steitz.** 1991. An intact box C sequence in the U3 snRNA is required for binding of fibrillarin, the protein common to the major family of nucleolar snRNPs. EMBO J. **10:**2645–2651.
5. **Beltrame, M., and D. Tollervey.** 1995. Base pairing between U3 and preribosomal RNA is required for 18S rRNA synthesis. EMBO J. **14:**4350–4356.
6. **Caffarelli, E., A. Fatica, S. Prislei, E. De Gregorio, P. Fragapane, and I. Bozzoni.** Processing of the intron-encoded U16 and U18 snoRNAs: the conserved C and D boxes control both the processing reaction and the stability of the mature snoRNA. EMBO J., in press.
7. **Cecconi, F., P. Mariottini, and F. Amaldi.** The *Xenopus* intron-encoded U17 snoRNA is produced by exonucleolytic processing of its precursor in oocytes. Nucleic Acids Res., in press.
8. **Cecconi, F., P. Mariottini, F. Loreni, P. Pierandrei-Amaldi, N. Campioni, and F. Amaldi.** $U17^{XS8}$, a small nucleolar RNA with a 12 nt complementarily to 18S rRNA and coded by a sequence repeated in the six introns of *Xenopus laevis* ribosomal protein S8 gene. Nucleic Acids Res. **22:**732–741.
9. **Chu, S., R. H. Archer, J. M. Zengel, and L. Lindahl.** 1994. The RNA of RNase MRP is required for normal processing of ribosomal RNA. Proc. Natl. Acad. Sci. USA **91:**659–663.
10. **Eichler, D. C., and N. Craig.** 1995. Processing of eukaryotic ribosomal RNA. Prog. Nucleic Acid Res. Mol. Biol. **49:**197–239.
11. **England, T. E., A. G. Bruce, and O. C. Uhlenbeck.** 1980. Specific labeling of 3′ termini of RNA with T4 RNA ligase. Methods Enzymol. **65:**65–74.
12. **Epstein, P., R. Reddy, and H. Busch.** 1984. Multiple states of U3 RNA in Novikoff hepatoma nucleoli. Biochemistry **23:**5421–5425.
13. **Filipowicz, W., and T. Kiss.** 1993. Structure and function of small nucleolar snRNPs. Mol. Biol. Rep. **18:**149–156.
14. **Fournier, M. J., and E. S. Maxwell.** 1993. The nucleolar snRNAs: catching up with the spliceosomal snRNAs. Trends Biochem. Sci. **18:**131–135.
15. **Goodall, G. J., K. Wiebauer, and W. Filipowicz.** 1990. Analysis of pre-mRNA processing in transfected plant protoplasts. Methods Enzymol. **181:**148–161.
16. **Hadjiolova, K., A. Normann, J. Cavaille, E. Soupene, S. Mazan, A. A. Hadjiolov, and J.-P. Bachellerie.** 1994. Processing of truncated mouse or human rRNA transcribed from ribosomal minigenes transfected into mouse cells. Mol. Cell. Biol. **14:**4044–4056.
17. **Hernandez, N.** 1992. Transcription of vertebrate snRNA genes and related genes, p. 281–313. *In* S. L. McKnight and K. R. Yamamoto (ed.), Transcriptional regulation. Cold Spring Harbor Laboratory Press, Cold Spring Harbor, N.Y.
18. **Huang, G. M., A. Jarmolowski, J. C. R. Struck, and M. J. Fournier.** 1992. Accumulation of U14 small nuclear RNA in *Saccharomyces cerevisiae* requires box C, box D, and a 5′, 3′ terminal stem. Mol. Cell. Biol. **12:**4456–4463.
19. **Hughes, J. M. X., and M. Ares, Jr.** 1991. Depletion of U3 small nucleolar RNA inhibits cleavage in the 5′ external transcribed spacer of yeast preribosomal RNA and prevents formation of 18S ribosomal RNA. EMBO J. **10:**4231–4239.
20. **Hügle, B., U. Scheer, and W. W. Franke.** 1985. Ribocharin: a nuclear M_r 40,000 protein specific to precursor particles of the large ribosomal subunit. Cell **41:**615–627.
21. **Kass, S., K. Tyc, J. A. Steitz, and B. Sollner-Webb.** 1990. The U3 small nucleolar ribonucleoprotein functions in the first step of preribosomal RNA processing. Cell **60:**897–908.
22. **Kawasaki, E. S., and A. M. Wang.** 1989. Detection of gene expression, p. 89–97. *In* H. A. Erlich (ed.), PCR technology. Principles and applications for DNA amplification. Stockton Press, New York.
23. **Kiss, T., and W. Filipowicz.** 1992. Evidence against a mitochondrial location of the 7-2/MRP RNA in mammalian cells. Cell **70:**11–20.
24. **Kiss, T., and W. Filipowicz.** 1993. Small nucleolar RNAs encoded by introns of the human cell cycle regulatory gene *RCC1*. EMBO J. **12:**2913–2920.
25. **Kiss, T., and Filipowicz.** 1995. Exonucleolytic processing of small nucleolar RNAs from pre-mRNA introns. Genes Dev. **9:**1411–1424.
26. **Kiss, T., C. Marshallsay, and W. Filipowicz.** 1991. Alteration of the RNA polymerase specificity of U3 snRNA genes during evolution and in vitro. Cell **65:**517–526.
27. **Kiss, T., C. Marshallsay, and W. Filipowicz.** 1992. 7-2/MRP RNAs in plant and mammalian cells: association with higher order structures in the nucleolus. EMBO J. **11:**3737–3746.
28. **Kiss, T., M. Tóth, and F. Solymosy.** 1985. Plant small nuclear RNAs. Nucleolar U3 snRNA is present in plants: partial characterization. Eur. J. Biochem. **152:**259–266.
29. **Konarska, M., W. Filipowicz, H. Domdey, and H. J. Gross.** 1981. Formation of a 2′-phosphomonoester, 3′,5′-phosphodiester linkage by a novel RNA ligase in wheat germ. Nature (London) **293:**112–116.
30. **Krol, A., and P. Carbon.** 1989. A guide for probing native small nuclear RNA and ribonucleoprotein structures. Methods Enzymol. **180:**212–227.
31. **Lerner, M. R., J. A. Boyle, J. A. Hardin, and J. A. Steitz.** 1981. Two novel classes of small ribonucleoproteins detected by antibodies associated with lupus erythematosus. Science **211:**400–402.
32. **Leverette, R. D., M. T. Andrews, and E. S. Maxwell.** 1992. Mouse U14 snRNA is a processed intron of the cognate *hsc70* heat shock protein premessenger RNA. Cell **71:**1215–1221.
33. **Li, H. V., J. Zagorski, and M. J. Fournier.** 1990. Depletion of U14 small nuclear RNA (snR128) disrupts production of 18S rRNA in *Saccharomyces cerevisiae*. Mol. Cell. Biol. **10:**1145–1152.
34. **Liang, W.-Q., and M. J. Fournier.** 1995. U14 base-pairs with 18S rRNA: a novel snoRNA interaction required for rRNA processing. Genes Dev. **9:**2433–2443.
35. **Lygerou, Z., P. Mitchell, E. Petfalski, B. Séraphin, and D. Tollervey.** 1994. The *POP1* gene encodes a protein component common to the RNase MRP and RNase P ribonucleoproteins. Genes Dev. **8:**1423–1433.
36. **Maxwell, E. S.** Personal communication.
37. **Maxwell, E. S., and M. J. Fournier.** 1995. The small nucleolar RNAs. Annu. Rev. Biochem. **35:**897–934.
38. **Montzka, K. A., and J. A. Steitz.** 1988. Additional low-abundance human small nuclear ribonucleoproteins: U11, U12, etc. Proc. Natl. Acad. Sci. USA **85:**8885–8889.
39. **Morrissey, J. P., and D. Tollervey.** 1993. Yeast snR30 is a small nucleolar RNA required for 18S rRNA synthesis. Mol. Cell. Biol. **13:**2469–2477.
40. **Morrissey, J. P., and D. Tollervey.** 1995. Birth of the snoRNPs: the evolution of RNase MRP and the eukaryotic pre-rRNA-processing system. Trends Biochem. Sci. **20:**78–82.
41. **Mougey, E. B., L. K. Pape, and B. Sollner-Webb.** 1993. A U3 small nuclear ribonucleoprotein-requiring processing event in the 5′ external transcribed spacer of *Xenopus* precursor rRNA. Mol. Cell. Biol. **13:**5990–5998.
42. **Nag, M. K., T. T. Thai, E. A. Ruff, N. Selvamurugan, M. Kunnimalaiyaan, and G. L. Eliceiri.** 1993. Genes for E1, E2, and E3 small nucleolar RNAs. Proc. Natl. Acad. Sci. USA **90:**9001–9005.
43. **Peculis, B. A., and J. A. Steitz.** 1993. Disruption of U8 nucleolar snRNA inhibits 5.8S and 28S rRNA processing in the *Xenopus* oocyte. Cell **73:**1233–1245.
44. **Peculis, B. A., and J. A. Steitz.** 1994. Sequence and structural elements critical for U8 snRNP function in *Xenopus* oocytes are evolutionarily conserved. Genes Dev. **8:**2241–2255.
45. **Reddy, R., and H. Busch.** 1988. Small nuclear RNAs: RNA sequences, structure, and modifications, p. 1–37. *In* M. L. Birnstiel (ed.), Structure and function of major and minor small nuclear ribonucleoprotein particles. Springer-Verlag, Berlin.
46. **Reimer, G., K. M. Pollard, C. A. Penning, R. L. Ochs, M. A. Lischwe, H. Busch, and E. M. Tan.** 1987. Monoclonal autoantibody from a (New Zealand

Black × New Zealand White) F1 mouse and some human scleroderma sera target an M_r 34,000 nucleolar protein of the U3 RNP particle. Arthritis Rheum. **30:**793–800.

47. **Rimoldi, O. J., B. Raghu, M. K. Nag, and G. L. Eliceiri.** 1993. Three new small nucleolar RNAs that are psoralen cross-linked in vivo to unique regions of pre-rRNA. Mol. Cell. Biol. **13:**4382–4390.
48. **Ruff, E. A., O. J. Rimoldi, B. Raghu, and G. L. Eliceiri.** 1993. Three small nucleolar RNAs of unique nucleotide sequences. Proc. Natl. Acad. Sci. USA **90:**635–638.
49. **Sambrook, J., E. F. Fritsch, and T. Maniatis.** 1989. Molecular cloning: a laboratory manual. Cold Spring Harbor Laboratory Press, Cold Spring Harbor, N.Y.
50. **Savino, R., and S. A. Gerbi.** 1990. *In vivo* disruption of *Xenopus* U3 snRNA affects ribosomal RNA processing. EMBO J. **9:**2299–2308.
51. **Schmitt, M. E., and D. A. Clayton.** 1993. Nuclear RNase MRP is required for correct processing of pre-5.8S rRNA in *Saccharomyces cerevisiae*. Mol. Cell. Biol. **13:**7935–7941.
52. **Sollner-Webb, B.** 1993. Novel intron-encoded small nucleolar RNAs. Cell **75:**403–405.
53. **Sollner-Webb, B., K. T. Tycowski, and J. A. Steitz.** Ribosomal RNA processing in eukaryotes. *In* A. E. Dahlberg and R. A. Zimmerman (ed.), Ribosomal RNA: structure, evolution, processing and function in protein synthesis, in press. CRC Press, Boca Raton, Fla.
54. **Tollervey, D.** 1987. A yeast small nuclear RNA is required for normal processing of pre-ribosomal RNA. EMBO J. **6:**4169–4175.
55. **Triglia, T., M. G. Peterson, and D. J. Kemp.** 1988. A procedure for *in vitro* amplification of DNA segments that lie outside the boundaries of known sequences. Nucleic Acids Res. **16:**8186.
56. **Tyc, K., and J. A. Steitz.** 1989. U3, U8 and U13 comprise a new class of mammalian snRNPs localized in the cell nucleolus. EMBO J. **8:**3113–3119.
57. **Tycowski, K. T., M.-D. Shu, and J. A. Steitz.** 1993. A small nucleolar RNA is processed from an intron of the human gene encoding ribosomal protein S3. Genes Dev. **6:**1120–1130.
58. **Tycowski, K. T., M.-D. Shu, and J. A. Steitz.** 1994. Requirement for intron-encoded U22 small nucleolar RNA in 18S ribosomal RNA maturation. Science **266:**1558–1561.
59. **Tycowski, K. T., and J. A. Steitz.** Personal communication.
60. **Venema, J., and D. Tollervey.** Processing of pre-ribosomal RNA in Saccharomyces cerevisiae. Yeast, in press.
61. **Warner, J. R.** 1990. The nucleolus and ribosome formation. Curr. Biol. **2:**521–527.
62. **Willis, I. M.** 1993. RNA polymerase III. Genes, factors and transcriptional specificity. Eur. J. Biochem. **212:**1–11.